Neuron, Vol. 48, 123–137, October 6, 2005, Copyright ©2005 by Elsevier Inc. DOI 10.1016/j.neuron.2005.09.005

Gene Expression Profiling of Facilitated L-LTP in VP16-CREB Mice Reveals that BDNF Is Critical for the Maintenance of LTP and Its Synaptic Capture

Angel Barco,[1,4,*] Susan Patterson,[1,6,7] Juan M. Alarcon,[1,7] Petra Gromova,[4] Manuel Mata-Roig,[5] Alexei Morozov,[1,2,8] and Eric R. Kandel[1,2,3]

[1]Center for Neurobiology and Behavior
[2]Howard Hughes Medical Institute and
[3]Kavli Institute for Brain Sciences
Columbia University
1051 Riverside Drive
New York, New York 10032
[4]Instituto de Neurociencias de Alicante
Universidad Miguel Hernandez
San Juan de Alicante 03550
Spain
[5]Unidad Central de Investigación
Facultad de Medicina
Universidad de Valencia
Valencia 46010
Spain
[6]Department of Psychology and
Center for Neuroscience
University of Colorado
Muenzinger D244
345 UCB
Boulder, Colorado 80309

Summary

Expression of VP16-CREB, a constitutively active form of CREB, in hippocampal neurons of the CA1 region lowers the threshold for eliciting the late, persistent phase of long-term potentiation (L-LTP) in the Schaffer collateral pathway. This VP16-CREB-mediated L-LTP differs from the conventional late phase of LTP in not being dependent on new transcription. This finding suggests that in the transgenic mice the mRNA transcript(s) encoding the protein(s) necessary for this form of L-LTP might already be present in CA1 neurons in the basal condition. We used high-density oligonucleotide arrays to identify the mRNAs differentially expressed in the hippocampus of transgenic and wild-type mice. We then explored the contribution of the most prominent candidate genes revealed by our screening, namely *prodynorphin*, *BDNF*, and MHC class I molecules, to the facilitated LTP of VP16-CREB mice. We found that the overexpression of brain-derived neurotrophic factor accounts for an important component of this phenotype.

Introduction

The encoding of new memories in the brain is thought to depend on long-lasting changes in the strength of synaptic connections between neurons, a change that depends, in turn, on transient or permanent alterations in specific patterns of gene expression. A number of transcription factors have been identified that play important roles during learning-related synaptic plasticity. Of these, the best-studied factor is the cAMP-responsive element binding protein CREB (reviewed in Barco et al., 2003; Lonze and Ginty, 2002). There is increased phosphorylation of CREB following stimuli that produce memory-related long-term potentiation (LTP) (Bito et al., 1996) as well as after training on hippocampus-dependent tasks (Taubenfeld et al., 1999). Similarly, the late phase of LTP and long-term memory storage correlate with increased cAMP responsive element (CRE)-dependent gene expression, as monitored via the activity of a CRE-driven *lacZ* reporter construct in transgenic mice (Impey et al., 1996, 1998).

To explore the role of CRE-driven genes in hippocampal synaptic plasticity, we generated transgenic mice in which we could induce, in a regulated manner and restricted to forebrain neurons, the expression of VP16-CREB, a constitutively active CREB protein. In the pyramidal cells of the CA1 region, the postsynaptic neurons of the Schaffer collateral pathway, VP16-CREB binds to CRE sites, regulates transcription of a number of CREB-dependent genes, and facilitates the establishment of L-LTP in a transcription-independent way. Based on these results we proposed a model in which VP16-CREB activates the transcription of CRE-driven genes and leads to a cell-wide distribution of proteins or mRNAs that prime synapses so that even a relatively weak stimulus will give rise to a long-lasting form of LTP (Barco et al., 2002).

To identify gene products upregulated in VP16-CREB mice that are responsible for the rapid consolidation of the long-term process following even a relatively weak stimulus, we carried out an analysis of altered gene expression in the hippocampus of these mice by using Affymetrix high-density oligonucleotide arrays. We identified mRNA transcripts differentially expressed in the hippocampus of transgenic and wild-type mice and then combined pharmacological and genetic approaches to investigate the possible contributions of the most prominent candidate genes in facilitating the L-LTP in the Schaffer collateral pathway of VP16-CREB mice.

Results and Discussion

Identification of Genes Whose Altered Expression in the Hippocampus of VP16-CREB Mice Correlates with the Facilitated L-LTP in the Schaffer Collateral Pathway

To better characterize the facilitated L-LTP phenotype of VP16-CREB mice, we carried out a time course analysis of the onset and reversion of this phenotype. We found that it was possible to switch transgene expression on and off in the hippocampus of mutant mice over the course of a week by controlling the presence of doxycycline (dox) in the animals' diet and at the

*Correspondence: abarco@umh.es
[7]These authors contributed equally to this work.
[8]Present address: Unit of Behavioral Genetics, NIMH, Building 49, Convent Drive, MSC Bethesda, Maryland 20892-4405.

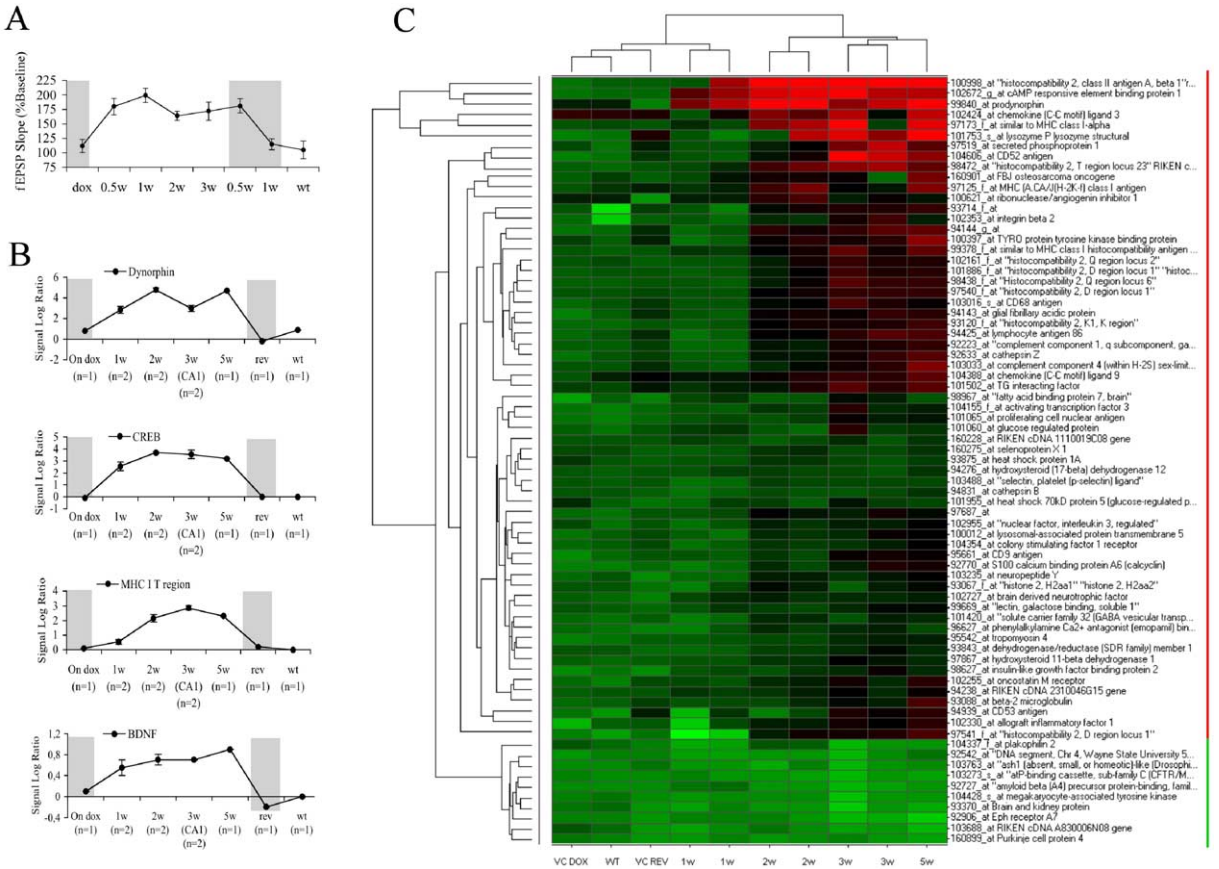

Figure 1. Time Course of Facilitated L-LTP Phenotype and Candidate Genes Induction

Gray boxes indicate the presence of dox in the mouse diet at the time of performing the experiment. Values are presented as means ± SEM. (A) The appearance of the LTP phenotype correlates with the induction of the VP16-CREB transgene (n = 6 slices [4 mice] per time point). The graph presents the average amplitude responses 110–130 min after delivering one 100 Hz train stimulation (1 s, 900 pulses). This stimulation protocol elicits E-LTP in wild-type mice, but L-LTP in VP16-CREB transgenics. (B) Time course of candidate gene upregulation: we used 81 transgenics and 26 wild-type mice divided into 12 different groups (in average, nine mice per group). The final data set included gene chips for animals on dox; 1, 2, 3 (microdissected CA1 regions), and 5 weeks after doxycycline removal; mice that expressed VP16-CREB for 3 weeks before turning transgene off again for 2 weeks (rev), and wild-type littermates (WT, n = 1 because one of the samples from whole hippocampus and the sample from microdissected CA1 regions were used as baseline). (C) Two-dimensional hierarchical clustering of ten samples and 73 genes, selected to include only those genes that were consistently changed in VP16-CREB mice after transgene induction but were unaltered in the different control situations (WT, DOX, and REV). See filter details in Table 1 legend. Two samples corresponding to wild-type mice (obtained from whole hippocampi or microdissected CA1 regions, respectively) were used for normalization and could not be included in this clustering.

same time that it was possible to regulate the LTP phenotype (Figure 1A).

To identify the specific genes whose induction in hippocampal neurons correlated with the facilitated L-LTP phenotype, we harvested hippocampal mRNA at time points assessed in our physiological study and carried out a gene expression analysis with the use of oligonucleotide microarrays. To obtain a sufficient quantity of poly(A)-RNA and reduce the effect of the biological variability of the sample, hippocampi from six to ten mice matched for genotype and time of induction were pooled together in each sample. The final data set included gene chips for animals on dox (gene Off) and for animals that had been removed from dox (gene ON) for 1, 2, and 5 weeks. We also included samples from wild-type mice maintained under identical conditions and from transgenic mice that expressed VP16-CREB for 3 weeks before turning the transgene off again for 2 weeks with dox (Rev, gene Off). Because the isolation of mRNA from the whole hippocampus favors genes that are more broadly overexpressed in the hippocampus of transgenic mice and, therefore, may lead to an underestimation of the total complement of genes showing an altered expression in specific hippocampal subregions, we extended our comparison between transgenic and wild-type expression profiles by using microdissected CA1 regions. We obtained two samples corresponding to VP16-CREB mice 3 weeks after induction and one sample corresponding to wild-type mice kept in the same conditions.

These mRNA samples were analyzed with Affymetrix gene chips MG-U74v2 setA, which allow the simultaneous analysis of 12,654 probe sets representing full-length mouse genes and Expressed Sequence Tag

(EST) clusters from the UniGene database (Build 74). We filtered and sorted the data through several sequential analyses by using the GCOS software package from Affymetrix. The *change p value* algorithm provides a measure of the likelihood of change and direction and is used to generate discrete *change calls*: *I* (increase), *MI* (marginal increase), *NC* (no change), *D* (decrease), and *MD* (marginal decrease). In our analysis, we demanded that the *change call* for all of those samples in which VP16-CREB expression was turned on (seven samples) indicated a statistically significant change in expression (i.e., *I*, *MI*, *D*, or *MD*). In addition, we also requested that the *change call* for wild-type samples or for those samples in which VP16-CREB expression was turned off was *NC*. Using this procedure, a surprisingly small list of only four genes emerged (Figure 1B and Table 1, first four rows). Notably, among these candidates was CREB itself, two well-known CREB-dependent genes (dynorphin and BDNF), and one MHC class I antigen.

We sorted these candidate genes using the *signal log ratio* (SLR), which estimates the magnitude and direction of the change. SLR values are expressed as the log2 ratio of the change in expression level between a baseline and an experiment array. First on our list, with the largest change, 13-fold on average, was the probe set targeted to *prodynorphin*, a gene that we had previously identified as being upregulated in VP16-CREB mice (Barco et al., 2002). In second place, we found a probe set targeted to *CREB* that recognizes a sequence present in both endogenous CREB and chimeric VP16-CREB mRNAs. Because the analysis of protein extracts from transgenic mice did not show any apparent change in the level of expression of endogenous CREB (Barco et al., 2002), the upregulation detected by the CREB probe likely corresponds to the induction of VP16-CREB transcripts. We cannot however exclude some contribution of the endogenous CREB transcripts, because the *CREB* promoter contains three CRE sites that confer positive *cis*-autoregulation. The presence of the CREB probe set in this restricted list of altered genes represented a valuable control that validated our analysis. The third probe set in our list recognizes transcripts encoding an isoform of MHC class I antigen. Class I MHC molecules are encoded by a large and highly homologous gene family whose role in regulating the immune response is well known and that has more recently also been found to be involved in synaptic plasticity (reviewed in Boulanger and Shatz, 2004). Finally, at the bottom of our list was BDNF. Although the change in BDNF mRNA was relatively small, it paralleled VP16-CREB expression in all of our samples.

Our initial highly restrictive criterion was designed to identify a small number of VP16-CREB target genes. By using a less restrictive criterion for sorting the data, we obtained a larger list of genes affected by the induction of VP16-CREB (Table 1). The hierarchical clustering of these probe sets revealed a good correlation between the altered expression of candidate genes and time after transgene induction. The clustering also highlighted the similarity of the expression profiles of samples from whole hippocampi and microdissected CA1 regions (Figure 1C). The extended list of candidate genes included a number of genes related to neuronal function and metabolism, such as c-*fos*, calcyclin, the vesicular GABA and glycine transporter, and neuropeptide Y. It is possible that additional genes that are differentially regulated in VP16-CREB mice escaped our screen because the microarray MG-U74A does not interrogate the complete mouse genome.

In a given cell, only a subset of the CRE sites in its genome is readily available for the binding of CREB and other CRE binding transcription factors, although the transactivation activity of bound CREB will remain low until the cell is exposed to extracellular stimuli that trigger its phosphorylation and the recruitment to the promoter of its coactivator CBP (Lonze and Ginty, 2002). When the chimeric transcription factor VP16-CREB binds to these available CRE sites in neurons of transgenic mice in the basal conditions, no additional extracellular stimuli are necessary to trigger the transcription of these promoters. Table 1 should, therefore, include such a subset of CRE-driven genes. Conversely, those CRE-driven genes that require additional signals to converge on their promoter to recruit CREB and trigger transcription would escape this screening approach.

The information available on the promoters of a number of candidate genes supports this view. Thus, the promoter of the *Pdyn* gene contains three consensus CRE sites and one nonconventional CRE site (Collins-Hicok et al., 1994) that participate in the regulation of the expression of dynorphin both in vivo and in vitro (Carlezon et al., 1998; Cole et al., 1995). Similarly, the mouse *MHC class I* promoter also contains two CRE-like sequences in the 5′ flanking region that are highly conserved among species and important for the expression and regulation of *MHC class I* genes by CREB (Ishiguro et al., 1998). The *BDNF* promoter also contains a consensus CRE and CRE-like sequences, and a number of experiments both in vivo and in vitro have previously shown that BDNF is regulated by CREB (Tabuchi et al., 2002; Tao et al., 1998). One CRE site has been identified in the promoter of *c-fos* and three in that of *CREB*.

It is also possible that some of the genes detected in our analysis are indirect targets of CREB. The identification of several transcription factors that are upregulated in VP16-CREB mice, including the immediate early response genes (IEG) c-*fos*, a well-known gene induced by neuronal activity, suggests that there may exist a second wave of transcriptional activation triggered by VP16-CREB induction. Notably, Table 1 also contains more than a dozen probes targeted to MHC class I antigen sequences, both classical and nonclassical. In addition to MHC class I antigens, we also found that other genes related to immune and inflammatory response were upregulated during the course of our experiment. It is difficult, however, to know whether the induction of these genes is a direct consequence of the activity of VP16-CREB or a side effect of the upregulation of MHC I observed at early time points. We are currently investigating the long-term consequences of this altered expression on neuronal survival.

Validation of Gene Chip Results by In Situ Hybridization

We used in situ hybridization to assess the expression of a number of interesting candidate and control genes.

Table 1. Genes with Altered Expression in the Hippocampus of VP16-CREB Mice

Score	Probe Set	Gene Name	SLR ± SD control(3)	SLR ± SD 1w(2)	SLR ± SD 2w(2)	SLR ± SD 3wCA1(2)	SLR 5w(1)	Function
0/7	99840_at	*Prodynorphin*	0.5 ± 0.6	2.8 ± 0.5	4.8 ± 0.3	3.0 ± 0.4	4.7	CC, N
0/7	102672_g_at	*cAMP responsive element binding protein 1*	0.0 ± 0.1	2.6 ± 0.5	3.7 ± 0.1	3.6 ± 0.5	3.2	TR
0/7	98472_at	*H2-T23: histocompatibility 2. T region locus 23*	0.1 ± 0.1	0.6 ± 0.2	2.2 ± 0.4	2.8 ± 0.2	2.3	ST
0/7	102727_at	*Brain derived neurotrophic factor*	0.0 ± 0.2	0.6 ± 0.2	0.7 ± 0.1	0.7 ± 0.0	0.9	CC, N
0/6	97173_f_at	*LOC436489: similar to MHC class I-alpha*	0.3 ± 0.1	0.6 ± 0.2	2.8 ± 0.4	2.4 ± 2.6	3.7	ST
1/6	103016_s_at	*CD68 antigen*	0.3 ± 0.3	0.3 ± 0.0	1.2 ± 0.1	1.8 ± 0.3	1.3	NA
0/6	96627_at	*Phenylalkylamine Ca^{2+} antagonist binding protein*	–0.1 ± 0.1	0.0 ± 0.4	0.6 ± 0.1	0.8 ± 0.1	0.4	CM
1/6	93088_at	*β-2 microglobulin*	0.2 ± 0.3	0.3 ± 0.1	0.6 ± 0.2	1.0 ± 0.1	2.0	ST
0/6	98627_at	*Insulin-like growth factor binding protein 2*	–0.2 ± 0.1	0.4 ± 0.1	0.4 ± 0.2	1.0 ± 0.4	0.7	NA
0/6	99669_at	*Lectin. galactose binding. soluble 1*	0.1 ± 0.1	0.4 ± 0.3	0.4 ± 0.1	0.9 ± 0.3	1.1	CD
–1/6	98967_at	*Fatty acid binding protein 7. brain*	–0.2 ± 0.4	0.5 ± 0.1	0.2 ± 0.1	1.0 ± 0.1	0.3	T
0/5	100998_at	*H2-Ab1: histocompatibility 2.*	0.0 ± 0.1	1.6 ± 2.0	4.2 ± 0.1	4.7 ± 0.4	4.9	ST
0/5	102424_at	*Chemokine (C-C motif) ligand 3*	1.7 ± 0.1	0.9 ± 0.8	2.4 ± 0.4	2.2 ± 1.5	3.3	CC, ST
0/5	97125_f_at	*LOC56628: MHC (A.CA/J(H-2K-f) class I*	0.6 ± 0.3	0.7 ± 0.1	2.2 ± 0.4	1.1 ± 0.1	2.6	NA
0/5	100621_at	*Ribonuclease/angiogenin inhibitor 1*	0.4 ± 0.8	0.9 ± 0.0	1.8 ± 0.2	1.1 ± 0.3	1.0	NA
1/5	101753_s_at	*Lysozyme*	0.4 ± 1.0	0.1 ± 0.4	1.7 ± 2.1	3.2 ± 0.7	5.9	CM
1/5	94144_g_at	*Similar to glial fibrillary acidic protein*	0.2 ± 0.4	0.1 ± 0.1	1.6 ± 0.1	2.0 ± 0.2	2.3	NA
1/5	100397_at	*TYRO protein tyrosine kinase binding protein*	0.5 ± 0.4	0.0 ± 0.1	1.5 ± 0.3	1.6 ± 0.1	2.7	NA
0/5	104388_at	*Chemokine (C-C motif) ligand 9*	0.8 ± 0.4	1.0 ± 0.0	1.4 ± 0.2	1.8 ± 0.1	2.3	CC, ST
1/5	160901_at	*c-fos (FBJ osteosarcoma oncogene)*	0.2 ± 0.2	0.7 ± 0.4	1.4 ± 0.0	0.6 ± 0.9	2.5	TR
0/5	99378_f_at	*LOC436493 (similar to MHC class I, H-2 Q4)*	0.2 ± 0.1	0.6 ± 0.1	1.4 ± 0.2	1.9 ± 0.6	2.3	NA
1/5	93120_f_at	*H2-K1: histocompatibility 2. K1. K region*	0.1 ± 0.2	0.2 ± 0.1	1.4 ± 0.2	1.6 ± 0.1	1.9	ST
1/5	94143_at	*Glial fibrillary acidic protein*	0.2 ± 0.5	0.2 ± 0.1	1.4 ± 0.1	1.6 ± 0.4	1.7	C&E
0/5	101502_at	*TG interacting factor*	0.6 ± 0.3	0.8 ± 0.2	1.3 ± 0.4	2.0 ± 0.4	2.2	TR
0/5	93714_f_at	*Similar to MHC class I*	–0.2 ± 1.0	0.1 ± 0.4	1.3 ± 0.3	1.6 ± 0.0	1.8	NA
1/5	97540_f_at	*H2-D1: histocompatibility 2. D region locus 1*	0.3 ± 0.1	0.2 ± 0.1	1.3 ± 0.1	1.8 ± 0.0	1.8	ST
0/5	104606_at	*CD52 antigen*	0.1 ± 0.4	0.2 ± 0.1	1.2 ± 0.3	3.7 ± 0.3	2.7	NA
1/5	94425_at	*Lymphocyte antigen 86*	0.3 ± 0.4	0.0 ± 0.1	1.2 ± 0.0	1.9 ± 0.3	2.0	CC
0/5	102161_f_at	*H2-Q2: histocompatibility 2. Q region locus 2*	0.2 ± 0.2	0.2 ± 0.1	1.2 ± 0.4	1.7 ± 0.1	1.6	ST
0/5	97541_f_at	*H2-D1: histocompatibility 2. D region locus 1*	–0.3 ± 0.3	–1.4 ± 0.4	1.1 ± 0.4	1.6 ± 0.1	2.0	ST
0/5	98438_f_at	*H2-Q7: histocompatibility 2. Q region locus 6*	0.2 ± 0.1	0.2 ± 0.1	1.1 ± 0.3	2.0 ± 0.3	1.8	ST
0/5	97687_at	*EST03336*	0.0 ± 0.2	0.4 ± 0.1	1.1 ± 0.1	1.2 ± 0.4	1.1	NA
1/5	97519_at	*Secreted phosphoprotein 1*	0.4 ± 0.5	0.3 ± 0.0	1.0 ± 0.2	2.9 ± 0.6	2.2	CC, ST
0/5	101886_f_at	*H2-D1: histocompatibility 2. D region locus 1*	0.2 ± 0.1	0.2 ± 0.1	1.0 ± 0.2	1.8 ± 0.2	1.7	ST
0/5	92633_at	*Cathepsin Z*	0.2 ± 0.3	0.1 ± 0.0	1.0 ± 0.0	1.6 ± 0.2	2.1	CM
0/5	93067_f_at	*Histone 2. H2aa1*	0.1 ± 0.2	0.1 ± 0.4	1.0 ± 0.2	0.5 ± 0.6	1.1	NA
1/5	92223_at	*C1qg (complement component 1γ)*	0.2 ± 0.2	0.0 ± 0.0	1.0 ± 0.1	1.5 ± 0.1	1.8	CC
1/5	103033_at	*Complement component 4 (within H-2S)*	0.4 ± 0.3	0.2 ± 0.1	0.9 ± 0.3	1.6 ± 0.2	2.6	CC
–1/5	103235_at	*Neuropeptide Y*	0.0 ± 0.3	0.0 ± 0.0	0.8 ± 0.1	0.8 ± 0.3	1.2	CC, ST
0/5	102330_at	*Allograft inflammatory factor 1*	–0.2 ± 0.6	–0.4 ± 1.1	0.8 ± 0.1	1.4 ± 0.2	1.7	S&C
0.5/5	102255_at	*Oncostatin M receptor*	0.1 ± 0.3	0.4 ± 0.1	0.8 ± 0.1	1.0 ± 0.5	1.7	CC, ST
0/5	94238_at	*RIKEN cDNA 2310046G15 gene*	0.2 ± 0.1	0.6 ± 0.1	0.8 ± 0.2	1.0 ± 0.4	1.3	CM
0/5	102955_at	*Nfil3: nuclear factor. interleukin 3. regulated*	0.2 ± 0.3	0.1 ± 0.3	0.8 ± 0.2	0.9 ± 0.0	1.2	CM
0/5	101420_at	*Slc32a1 (GABA vesicular transporter)*	0.0 ± 0.1	–0.1 ± 0.1	0.7 ± 0.0	0.6 ± 0.4	0.7	T
0/5	160275_at	*Selenoprotein X 1*	0.3 ± 0.2	0.2 ± 0.1	0.7 ± 0.1	0.4 ± 0.0	0.6	CM
0/5	102353_at	*Integrin β2*	–0.3 ± 0.7	0.1 ± 0.1	0.7 ± 0.1	1.6 ± 0.4	0.9	CC, ST
1/5	100012_at	*Lysosomal-associated protein transmembrane 5*	0.1 ± 0.3	0.0 ± 0.1	0.6 ± 0.1	1.0 ± 0.4	1.2	NA
0/5	97867_at	*Hydroxysteroid 11-beta dehydrogenase 1*	0.1 ± 0.1	0.2 ± 0.0	0.6 ± 0.0	1.1 ± 0.1	0.7	CM
1/5	93875_at	*Heat shock protein 1A*	0.3 ± 0.3	0.2 ± 0.1	0.6 ± 0.0	0.3 ± 0.1	0.5	CM
0/5	92770_at	*S100 calcium binding protein A6 (calcyclin)*	–0.1 ± 0.1	–0.1 ± 0.1	0.6 ± 0.2	1.2 ± 0.6	1.4	ST
1/5	104354_at	*Csf1r: colony stimulating factor 1 receptor*	0.2 ± 0.2	0.0 ± 0.1	0.6 ± 0.1	0.8 ± 0.2	1.2	CC, ST
0/5	104155_f_at	*Atf3: Activating transcription factor 3*	–0.1 ± 0.1	0.2 ± 0.1	0.6 ± 0.1	1.2 ± 0.7	0.9	TR
1/5	95661_at	*CD9 antigen*	0.0 ± 0.3	0.2 ± 0.1	0.5 ± 0.1	1.4 ± 0.1	1.3	CC
0/5	93843_at	*Dhrs1: dehydrogenase/reductase SDR1*	0.1 ± 0.1	0.1 ± 0.1	0.5 ± 0.0	0.9 ± 0.3	0.7	CM

(*continued*)

Table 1. Continued

Score	Probe Set	Gene Name	SLR ± SD control(3)	SLR ± SD 1w(2)	SLR ± SD 2w(2)	SLR ± SD 3wCA1(2)	SLR 5w(1)	Function
0/5	94276_at	*Hydroxysteroid (17-beta) dehydrogenase 12*	0.2 ± 0.1	0.4 ± 0.2	0.4 ± 0.1	0.4 ± 0.1	0.6	CM
0/5	103488_at	*Selectin. platelet (p-selectin) ligand*	0.2 ± 0.1	–0.1 ± 0.1	0.4 ± 0.1	0.4 ± 0.0	0.4	CC
0/5	95542_at	*Tropomyosin 4*	–0.1 ± 0.2	0.2 ± 0.1	0.4 ± 0.0	0.8 ± 0.1	0.8	C&E
0/5	101065_at	*Proliferating cell nuclear antigen*	–0.1 ± 0.1	0.4 ± 0.1	0.4 ± 0.2	1.0 ± 0.4	1.0	CM
0/5	94831_at	*Cathepsin B*	0.2 ± 0.1	0.0 ± 0.1	0.4 ± 0.1	0.3 ± 0.1	0.6	CM
1/5	101955_at	*Heat shock 70kD protein 5*	0.2 ± 0.4	0.3 ± 0.4	0.3 ± 0.3	0.8 ± 0.4	0.4	CC, CM
0/5	160228_at	*RIKEN cDNA 1110019C08 gene*	0.3 ± 0.0	0.4 ± 0.1	0.2 ± 0.2	0.5 ± 0.3	0.6	NA
0/5	101060_at	*Grp58: glucose regulated protein*	0.1 ± 0.2	0.6 ± 0.1	0.2 ± 0.2	1.1 ± 0.8	0.6	CM
1/5	94939_at	*CD53 antigen*	0.1 ± 0.6	–0.1 ± 1.0	0.1 ± 0.4	1.4 ± 0.2	1.7	NA
0/-5	103273_s_at	*Abcc8: ATP-binding cassette C8*	–0.3 ± 0.1	–0.3 ± 0.1	–0.6 ± 0.1	–0.6 ± 0.2	–0.6	ST
0/–5	103763_at	*Ash1-like*	–0.2 ± 0.1	–0.4 ± 0.0	–0.4 ± 0.4	–0.6 ± 0.3	–0.3	CM
–1/–5	160899_at	*Purkinje cell protein 4*	–0.3 ± 0.2	–0.4 ± 0.2	–0.4 ± 0.1	–0.3 ± 0.1	–0.6	NA
0/–5	92727_at	*Amyloid beta (A4) precursor protein-binding A2*	–0.3 ± 0.0	–0.1 ± 0.1	–0.4 ± 0.0	–0.7 ± 0.1	–0.5	T
–1/–5	92906_at	*Eph receptor A7*	–0.3 ± 0.2	–0.2 ± 0.0	–0.4 ± 0.2	–0.8 ± 0.1	–1.1	CC, ST
–1/–5	104428_s_at	*Megakaryocyte-associated tyrosine kinase*	–0.2 ± 0.1	–0.4 ± 0.1	–0.3 ± 0.0	–0.6 ± 0.4	–0.5	CC, CM
–1/–5	103688_at	*RIKEN cDNA A830006N08 gene*	–0.0 ± 0.4	–0.4 ± 0.2	–0.2 ± 0.1	–0.5 ± 0.1	–0.8	NA
1/–5	104337_f_at	*Plakophilin 2*	0.0 ± 0.2	–0.6 ± 0.1	0.2 ± 0.1	–0.6 ± 0.3	–0.4	CC
–1/–6	92542_at	*D4Wsu53e*	–0.3 ± 0.1	–0.6 ± 0.0	–0.4 ± 0.1	–0.6 ± 0.4	–0.1	NA
–1/–6	93370_at	*Brain and kidney protein*	–0.2 ± 0.2	–0.4 ± 0.3	–0.4 ± 0.0	–0.8 ± 0.4	–0.7	ST

Score (control/VC): We assigned the following values to the *change calls* produced by GCOS: I = 1, MI = 0.5, D = –1, MD = –0.5, and NC = 0. Then we added up the values obtained for control samples (control, values can rank from –3 to 3) and for samples in which VP16-CREB was expressed (VC, ranking from –7 to 7). Probe sets showing an altered expression that correlated exactly with the state of transgene activation should score 0/7 for increased expression or 0/–7 for decreased expression. This table shows those probes with a score for controls between –1 and 1, and a score for VC < –5 for downregulation or >5 for upregulation. SLR ± SD: Average of signal log ratio values (log2 ratio) ± standard deviation. Control: samples corresponding to wild-type mice or VP16-CREB mice on dox. 1w, 2w, 3w, 5w: VP16-CREB mice 1, 2, 3, or 5 weeks after dox removal. The number of samples per experimental group is indicated in brackets. Function: Biological or molecular functions based in Gene Ontology annotations: CC, cell communication; CD, cell differentiation; CM, cell metabolism; N, neurotransmission; S&C, structural and cytoskeleton; ST, signal transduction; T, transport; TR, transcriptional regulation; NA, no annotation.

We chose candidate genes based on our gene chip analysis or their previous identification as IEGs potentially regulated by CREB. The genes analyzed included *dynorphin*, *MHC I* genes, *c-fos*, *BDNF*, *junB*, *C/EBPβ*, *nur77*, *enkephalin*, *MKP1*, and *Arc* (Figure 2 and data not shown). Although the result of this analysis was, in general, consistent with the gene chip data, in the case of *junB* the in situ hybridization analysis revealed a CA1-restricted upregulation that did not pass GCOS statistical filters.

These experiments revealed an interesting feature of VP16-CREB-dependent gene expression: the response of different brain regions to the induction of constitutively active CREB protein was different. For some genes, such as those encoding MHC I antigens, the regional pattern of expression closely mirrored that of VP16-CREB, whereas for others the altered expression was restricted to a subset of cells. Thus, in the case of *prodynorphin*, the response in striatal neurons was amplified in comparison to hippocampal neurons, consistently with the natural pattern of expression of this gene, higher in striatum than in hippocampus, whereas IEGs, such as *BDNF*, *c-fos*, or *junB*, were highly expressed exclusively in the CA1 region of the hippocampus. These results suggest the contribution of epigenetic mechanisms, such as cell type-specific methylation of CRE sites, and region-specific transcription factors working together with CREB on the transcriptional regulation of these genes.

Functional Validation of Candidate Genes

We next combined pharmacological and genetic approaches to investigate the role of the three most prominent candidate genes (dynorphin, MHC I, and BDNF) in the enhanced form of L-LTP observed in VP16-CREB transgenic mice.

Prodynorphin Is Highly Overexpressed in CA1 Cells of VP16-CREB Mice but Is Not Required for the Enhanced L-LTP Phenotype

The gene *Pdyn* encodes prodynorphin, the precursor of several biologically active opioid peptides known as dynorphins. Although the role of prodynorphin in controlling pain and responses to stress in the peripheral nervous system has been studied extensively, its role in the central nervous system, including its possible role in learning and memory, is less understood. Two different modes of action have been suggested for dynorphins, one dependent on opioid receptors that is blocked by the antagonist naloxone, the other dependent on a nonopioid receptor that is resistant to naloxone and blocked by NMDA antagonists (Shukla and Lemaire, 1994). In the granular neurons of the dentate gyrus, dynorphin plays an inhibitory role in synaptic plasticity of the mossy fiber (Terman et al., 1994; Wagner et al., 1993). However, in the Schaffer collaterals terminating in the CA1 region, where κ-opioid receptors are absent, dynorphin appears to have dual effects on NMDA synaptic currents, increasing NMDA currents at low concentrations of dynorphin and decreasing these currents at high concentrations (Caudle et al., 1994).

To explore further the general role of dynorphin in hippocampal LTP in the Schaffer collateral pathway, we first tested the effect of bath-applied dynorphin (1-13) [Dyn(1-13)], a biologically active form of this neuropeptide. We found that Dyn(1-13) did not affect basal synaptic transmission (Figure 3A; 10 min before incubation,

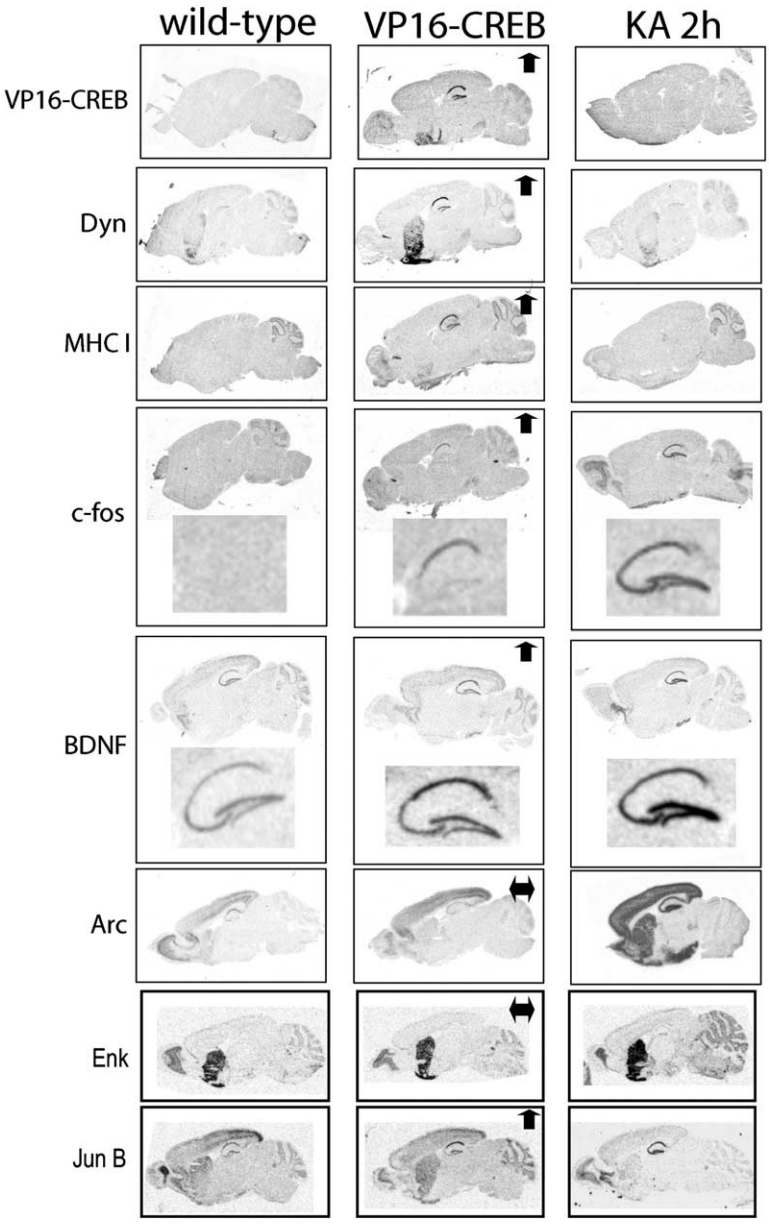

Figure 2. In Situ Hybridization of Candidate Genes

In situ hybridizations using oligo probes specific for the indicated genes on brain sagittal sections from VP16-CREB mice and wild-type littermates 2 weeks after dox removal. Sections from wild-type mice injected with kainic acid 2 hr before sacrificing (KA 2h) were used as positive control for IEG induction. Arrows in the central panels indicate the direction of the expression change. Our experiments show enhanced expression of several CRE-dependent genes (such as *prodynorphin*, MHC I, *c-fos*, *BDNF*, and *junB*); however, we did not see upregulation of *enkephalin* (also absent in the gene chip screen). *Arc* is shown here as negative control for an IEG gene not affected by VP16-CREB expression; interestingly, its promoter does not contain any CRE site. Similar results were obtained with three independent sets of animals.

percent baseline = 97% ± 3.8%; 20–30 min after Dyn (1-13) addition, percent baseline = 101% ± 4.9%; p = 0.11) or the duration of LTP induced by one train of 100 Hz stimulation (Figures 3A and 3B; 1–20 min, percent baseline = 189% ± 17.8% for control and 194% ± 17.6% for Dyn(1-13), p = 0.39; 100–115 min, percent baseline = 103% ± 2.2% for control and 105.8% ± 3% for Dyn(1-13), p = 0.11). There was however a transient increase in the amplitude of LTP after the peptide was removed from the bathing solution (30–60 min, percent baseline = 135% ± 10% for control and 156% ± 12.5% for Dyn(1-13), p = 0.034).

To carry this investigation further, we examined the consequences of depleting dynorphin. *Pdyn* knockout mice (*Pdyn*$^{-/-}$) are viable and show no apparent phenotypic alterations (Sharifi et al., 2001). We first tested whether basal synaptic plasticity in the Schaffer collateral pathway was affected in these mutants and found that the stimulus-response curve was similar in wild-type and knockout mice (Figure 3C, p = 0.39). Long-term depression (LTD) as well as both E-LTP and L-LTP, induced, respectively, by 1 Hz stimulation, one train of 100 Hz, or by four trains of 100 Hz stimulation, were also unaltered by the dynorphin deficiency (Figure 3D, LTD 60–90 min, percent baseline = 85% ± 4.79% for wild-type and 86% ± 4.22% for *Pdyn*$^{-/-}$; p = 0.11; Figure 3E, E-LTP 30–60 min, percent baseline = 123% ± 7.1% for wild-type and 130% ± 6.2% for *Pdyn*$^{-/-}$; p = 0.12; and Figure 3F, L-LTP 90–120 min, percent baseline = 171% ± 7.6% for wild-type and 180% ± 5.8% for *Pdyn*$^{-/-}$; p = 0.07). Dynorphin therefore does not appear to play a relevant role in these forms of synaptic plasticity in wild-type animals.

We next tested the consequences of dynorphin de-

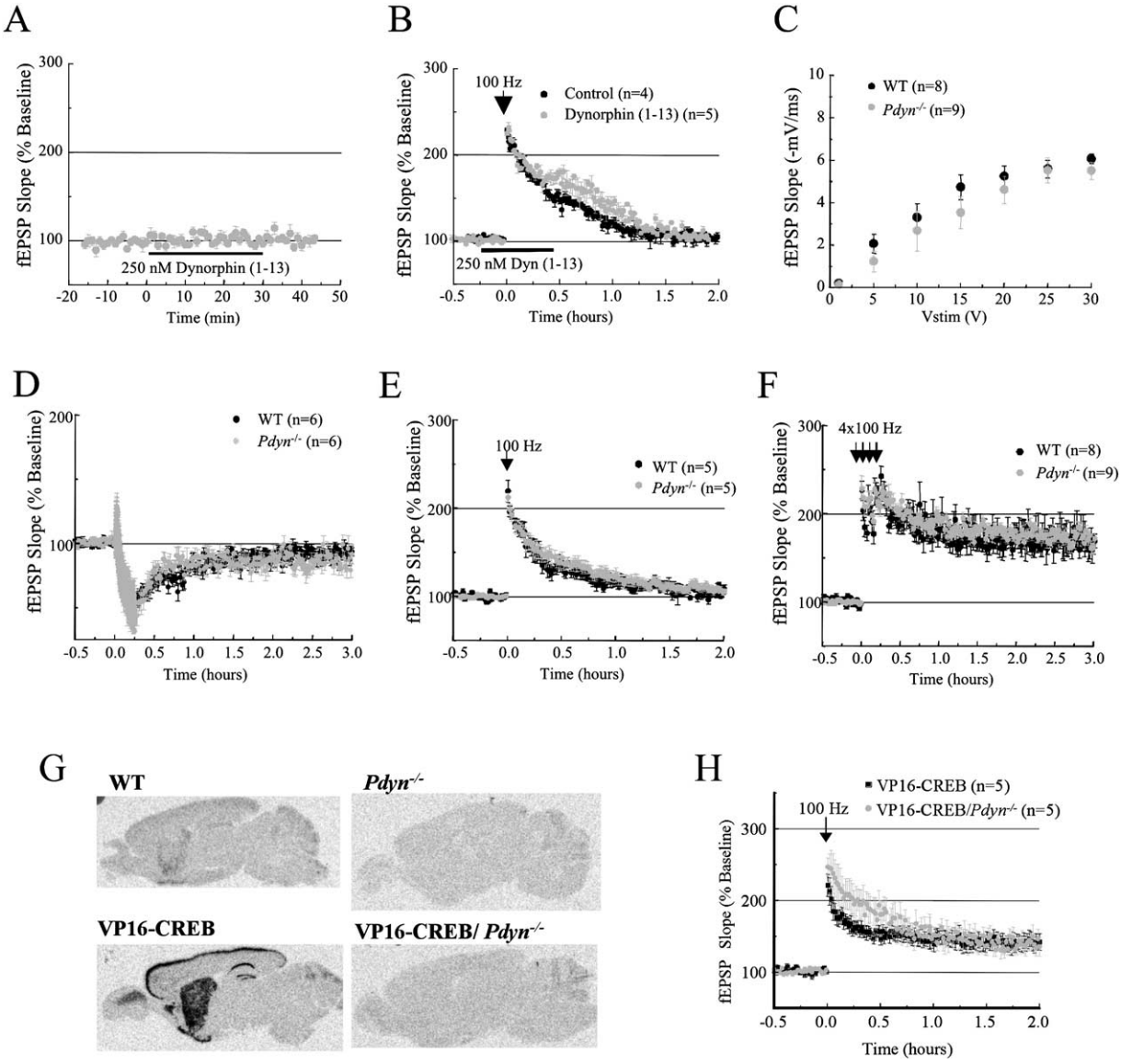

Figure 3. The Exogenous Addition or the Genetic Suppression of Dynorphin Does Not Affect Normal L-LTP nor Facilitated L-LTP in VP16-CREB Mice

Exogenous addition of dynorphin (250 nM) had no significant effect either on test fEPSPs generated at CA3-CA1 synapses of wild-type mice (A) or in the duration of E-LTP induced by a single tetanus of 100 Hz stimulation (B). (C) Input-output curve of fEPSP slope (mV/ms) versus stimulus (V) at the Schaffer collateral pathway of hippocampal slices from *Pdyn*$^{-/-}$ and control mice. (D) A 900 pulse train at 1 Hz evoked LTD in wild-type and mutant animals. (E) A single 100 Hz train (1 s) evoked E-LTP in wild-type and mutant animals. (F) Four 100 Hz train stimulation leads to L-LTP in both mutant and control mice. (G) In situ hybridization using an oligonucleotide probe specific for dynorphin shows that *Pdyn*$^{-/-}$ mice and VP16-CREB/*Pdyn*$^{-/-}$ double mutants do not express dynorphin mRNA, while VP16-CREB mice highly overexpress this mRNA in specific forebrain regions. (H) Expression of VP16-CREB favored the persistence of LTP induced by one 100 Hz train, even in the absence of dynorphin. In all panels, results were presented as means ± SEM.

pletion in VP16-CREB mice by crossing VP16-CREB mice with mice deficient in dynorphin expression. In the hippocampus of wild-type mice, the expression of dynorphin peptides is low in the granular cells of dentate gyrus and undetectable in CA1 and CA3 regions, whereas the staining of sections from VP16-CREB mice revealed that the same CA1 neurons that expressed VP16-CREB in the nucleus also overexpressed dynorphin in the cytoplasm (data not shown). As expected, *Pdyn*$^{-/-}$ and VP16-CREB/*Pdyn*$^{-/-}$ double mutants did not express dynorphin at all (Figure 3G).

Despite a lack of dynorphin expression, the induction of VP16-CREB in VP16-CREB/*Pdyn*$^{-/-}$ double mutants still led to a reduced threshold for L-LTP that was similar to that observed in VP16-CREB single mutant mice (Figure 3H, 60–90 min, percent baseline = 147% ± 6.2% for VP16-CREB mice and 143% ± 4.5% for VP16-CREB/*Pdyn*$^{-/-}$ mutants, p = 0.39), although L-LTP in

double mutants was significantly enhanced during its early expression (Figure 3H, 1–30 min, percent baseline = 169% ± 17% for VP16-CREB mice and 205% ± 20% for VP16-CREB/*Pdyn*$^{-/-}$ mice, p = 0.007). Thus, in spite of the fact that VP16-CREB greatly increases the expression of dynorphin, we could not correlate the activity of this protein to the LTP phenotype observed in VP16-CREB mice. The function and consequences of dynorphin upregulation in the CA1 region remain unknown.

MHC I Antigens Are Upregulated in Hippocampal Neurons of VP16-CREB Mice and Are Involved in L-LTP

Our screen for overexpressed genes in VP16-CREB mice revealed more than a dozen ESTs encoding MHC I antigens (Table 1). A role for MHC I molecules in synaptic plasticity was first suggested by an unbiased screen for genes involved in synaptic plasticity during development of the visual system (Corriveau et al., 1998). Based on that study, Shatz and colleagues proposed that MHC I expression had a postsynaptic role acting as a "synaptic glue" in stabilizing appropriate synaptic connections, a view consistent with our results in VP16-CREB mice. A subsequent study by Shatz and her colleagues examined the synaptic plasticity and LTP phenotype of mice deficient for MHC I signaling (Huh et al., 2000) and found that in these mutants the normal segregation of retinal afferent axons in central targets during development was disrupted and synaptic plasticity in hippocampal neurons of adult animals was altered. In particular, LTP in the Schaffer collateral pathway was enhanced and LTD was absent. Based on these new findings, Shatz and colleagues elaborated on their model, concluding that MHC I molecules may also promote the elimination, by pruning, of inappropriate synapses during development and in the adult. This hypothesis, therefore, suggests that the enhanced LTP observed in MHC I- deficient mice reflects an absence of the normal pruning of synaptic connections in the hippocampus during development (Huh et al., 2000).

To identify the MHC I variants expressed in the hippocampus of VP16-CREB mice, we performed RT-PCR of hippocampal mRNA by using primers targeted to a segment that varies considerably among different class members of the MHC I antigen family (see Table S1 in the Supplemental Data available online). We found that both wild-type and transgenic mice expressed multiple MHC I antigens in hippocampal neurons, although the level of expression for the different MHC I subfamilies, both classical and nonclassical, was higher in mutant mice (Figure 4A and data not shown).

As a first step in exploring the possible contribution of alterations in MHC I to the facilitated L-LTP observed in VP16-CREB mice, we analyzed the response to 100 Hz stimulation in the Schaffer collateral pathway of *CD3*$\delta^{-/-}$ mice (Love et al., 1993), one of the two MHC I-deficient strains used in Huh et al.'s study. CD3δ is a component of the class I MHC receptor that is expressed in many cell types, including neurons, and its depletion disrupts MHC I signaling. We found that a standard 100 Hz tetanus train of 1 s duration, which produces a nonsaturating short-lasting LTP (E-LTP) in wild-type mice, evoked an enhanced and subtained form of LTP in *CD3*$\delta^{-/-}$ mutants (Figure 4C, first 5 min, percent baseline = 167% ± 7% for wild-type mice and 196% ± 14% for *CD3*$\delta^{-/-}$ mice, p = 0.026; at 2 hr, percent baseline = 106% ± 2% for wild-type mice and 157% ± 6% for *CD3*$\delta^{-/-}$ mice, p = 0.0001). By contrast, the stimulus-response curve was not significantly altered in knockout mice (Figure 4B, p = 0.35). This enhanced response to 1 × 100 Hz stimulation is consistent with the enhanced response to 4 × 100 Hz stimulation reported by Huh and colleagues and attributed by them to the absence of pruning of synaptic connections during development. Since L-LTP is already facilitated in MHC I-deficient mutants, the introduction of VP16-CREB into a MHC I-deficient background would be unlikely to reveal additional information about the contribution of MHC I molecules to the enhanced phenotype. The exploration of the consequences of MHC I disruption on enhanced LTP in VP16-CREB mice will require the generation of mutant mice in which MHC I deficiency occurs in the adult brain, thus bypassing the developmental consequences of its early disruption.

MHC I antigens are expressed at low levels in the prenatal hippocampus, but their expression increases as hippocampal neurons mature, and these molecules may come to play a role in modulating adult synaptic plasticity (Boulanger et al., 2001). Although under normal circumstances the blood-brain barrier prevents the entry of leukocytes, antibodies, complement factors, and cytokines into the parenchyma of the brain, a significant increase in MHC I expression, such as in individuals with chronic epilepsy or after prolonged VP16-CREB expression, might make the expressing neurons more susceptible to destruction by invading cells of the immune system. The presence of cytokine mRNAs and other transcripts related to inflammatory processes in samples of VP16-CREB mice may reflect this phenomenon (Table 1).

BDNF: A Key Component of the Enhanced LTP Driven by VP16-CREB

The identification of *BDNF* in our unbiased screen for genes that are important in late-phase LTP reinforces the already strong evidence supporting a critical role for BDNF in some forms of L-LTP. Inhibition of endogenous BDNF or of the signaling through its TrkB receptor impairs the late phase of some forms of LTP, indicating that BDNF is required for its full expression (reviewed in Lu, 2003). Furthermore, BDNF expression increases after induction of LTP in the CA1 region of the hippocampus and after learning-related events (Lu, 2003; Patterson et al., 1992).

The genomic structure of the *BDNF* gene is unusually complex. This gene contains multiple promoters that drive the expression of transcripts bearing different noncoding exons spliced upstream of a common 3′ exon that encompasses the entire encoding sequence. The detailed characterization of the rat *BDNF* gene has revealed the existence of at least four promoters located upstream of these alternatively spliced exons that enable a precise regulation of BDNF expression in different cell types or in response to different stimuli (Timmusk et al., 1993). The structure of the mouse gene is very similar to that of rat (93% homology), but the mouse gene appears to contain an additional promoter

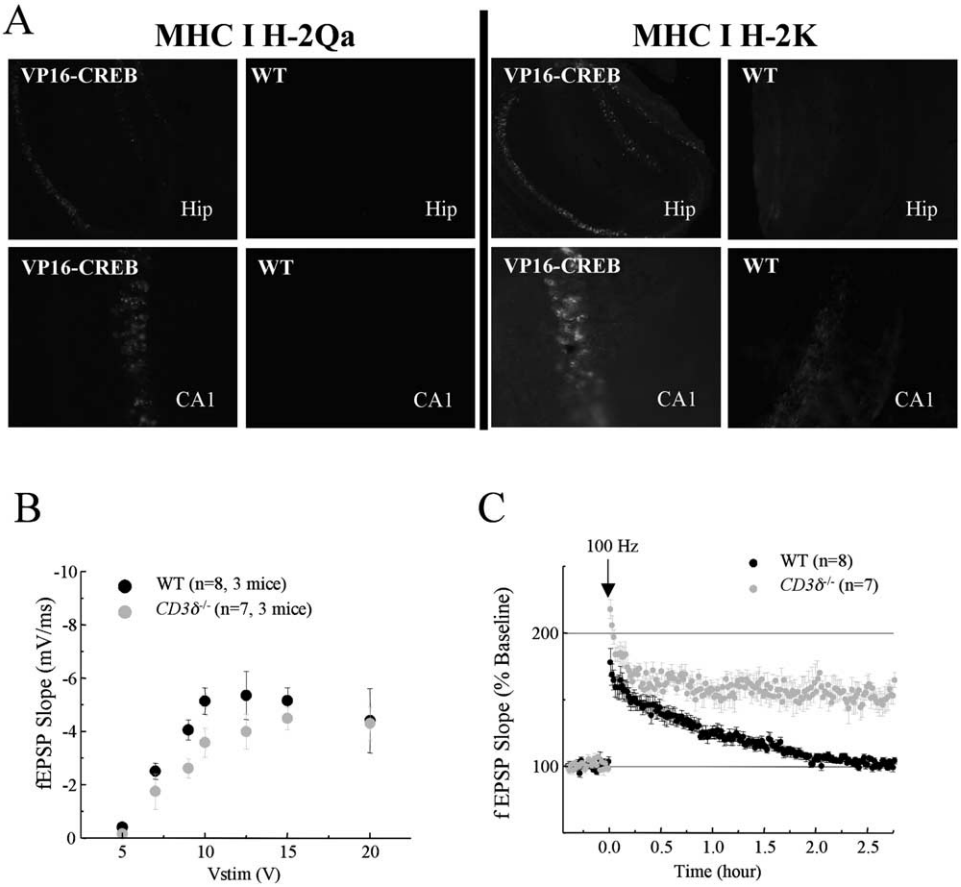

Figure 4. The Expression of Multiple MHC I Genes Is Upregulated in VP16-CREB Mice

(A) In situ hybridization analysis reveals the overexpression of two different MHC I variants in the hippocampus (upper panels) of a VP16-CREB mouse. Lower panels show a higher-magnification image of the CA1 region. (B) Input-output curve of fEPSP slope (mV/ms) versus stimulus (V) at the Schaffer collateral pathway of hippocampal slices from *CD3δ* $^{-/-}$ and control mice. (C) A single 100 Hz train evoked L-LTP in *CD3δ* $^{-/-}$ mice. Values are presented as means ± SEM.

and alternative exon located in a sequence homologous to rat intron II (Martinowich et al., 2003).

To identify the BDNF transcripts upregulated by VP16-CREB, we carried out a quantitative RT-PCR analysis with primer pairs specific for each one of the five upstream exons (Figure 5A). We found that the expression of mRNAs bearing exons 1, 2, and 3 were significantly increased in VP16-CREB mice whereas the expression of exons 4 and 5 were not affected (Figure 5B). Interestingly, exons 1, 2, and 3 are clustered within 1.5 kb at the 5′ end of the gene and 15 kb apart from exons 4 and 5. The analysis of the genomic sequence upstream of exon 1 has revealed the existence of regulatory elements responsible for the Ca^{2+}-mediated activation of PI (Tabuchi et al., 2000), including a CRE site that overlaps with a USF binding element (Tabuchi et al., 2002). CRE elements have also been reported upstream of PII, although their functionality has not been confirmed (Hayes et al., 1997). Previous studies on the rat *BDNF* gene suggested that the promoters PI and PII shared common regulatory elements. Indeed, a neural-restrictive silencer element (NRSE) located in intron 1 contributes to the regulation of both promoters (Timmusk et al., 1999). Because the molecular interactions that underlie the activation of transcription by VP16-CREB and phospho-CREB are different, the transactivation driven by the VP16 domain might have a broader range than that of CREB. It is therefore possible that the binding of VP16-CREB to the CRE element in PI also activates the expression driven by promoter PII and even PIII, which are located relatively close downstream of a functional CRE site but have not been previously reported as being regulated by CREB. Strikingly, we did not detect any effect of VP16-CREB expression on the expression of BDNF driven by promoter PIV, in spite of the presence of a conserved CRE site upstream of this promoter (Shieh and Ghosh, 1999; Tao et al., 1998). Experiments in rat neuronal cultures have found that membrane depolarization induces the transcription from both P1 and PIII (PIV in the mouse). Some of these experiments suggest that PIII responds to depolarization but not to an increase of internal cAMP (Tao et al., 2002), suggesting that the activation of CREB is not sufficient to drive rat BDNF PIII expression, a view that might explain our negative results for mouse promoter PIV.

To evaluate the component of the facilitated L-LTP in VP16-CREB mice that is due to an enhanced expres-

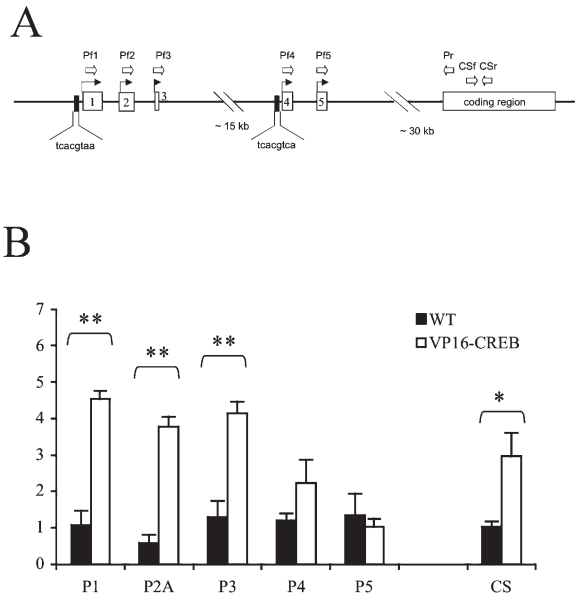

Figure 5. VP16-CREB Induces the Expression of BDNF Exons 1, 2, and 3

Real-time quantitative PCR was used to measure the expression of BDNF transcripts bearing the differentially regulated exons 1 to 5 in VP16-CREB mice 2 weeks after dox removal from the diet. (A) Schematic representation of the *BDNF* gene. The different exons are indicated by open boxes. Black arrows represent the different promoters, while the upper open arrows indicate the location of the different oligos used in this study. Black boxes represent the CRE sites upstream of promoters PI and PIV. (B) We found that the expression of exons 1, 2, and 3 were significantly upregulated in VP16-CREB mice, whereas the expression of exons 4 and 5 were not affected. Values are presented as means ± SEM. The amplification of a sequence located on the coding sequence (CS) common to all BDNF transcripts confirmed the upregulation detected in the Affymetrix analysis. Asterisks indicate significant differences from the control (*$p < 0.05$; **$p < 0.005$).

sion of BDNF we carried out two experiments. First, we incubated hippocampal slices from VP16-CREB mice and from wild-type littermates with the BDNF scavenger TrkB receptor body (TrkB-Fc). This protein scavenges unbound BDNF and blocks its interaction with cellular receptors. Although we observed normal E-LTP in wild-type mice in the presence of this protein (Figure 6A, 30–60 min, percent baseline = 146% ± 9.8% for control and 141% ± 16 for TrkB-Fc, $p = 0.17$), the late expression of the enhanced LTP of VP16-CREB mice was significantly reduced after incubation with TrkB-Fc (Figure 6B, 30–60 min, percent baseline = 189% ± 6.1% for control and 160% ± 12 for TrkB-Fc, $p = 0.025$).

Second, we crossed BDNF heterozygous mice (*BDNF*$^{+/-}$), in which expression of BDNF mRNA is reduced to about half the level of wild-type mice (Ernfors et al., 1994), with VP16-CREB transgenics. Unlike the experiments with *Pdyn*$^{-/-}$ and *CD3δ* $^{-/-}$ mice, we could not use *BDNF* homozygous mutants (*BDNF*$^{-/-}$), due to the early mortality and severe developmental problems of these mice. The reduction in BDNF levels in *BDNF*$^{+/-}$ mice did not alter the stimulus-response curves of either *BDNF*$^{+/-}$ or VP16-CREB /*BDNF*$^{+/-}$ mice (Figures 6C and 6D). Similarly to our experiments using TrkB-Fc, we found that genetic reduction of BDNF expression largely blocked the enhanced LTP phenotype observed in VP16-CREB mice but did not affect E-LTP in wild-type mice (Figure 6E, 3 hr post-tetanus, percent baseline = 134% ± 11% for wild-type mice and 135% ± 18% for *BDNF*$^{+/-}$ mice, $p = 0.98$; Figure 6F, 3 hr post-tetanus, percent baseline = 186% ± 21% for VP16-CREB mice and 126% ± 9% for VP16-CREB/*BDNF*$^{+/-}$ mice, $p < 0.03$).

These two experiments taken together strongly indicate that a significant component contributing to the L-LTP phenotype of VP16-CREB mice results from overexpression of BDNF.

A Predicted Role of BDNF in Synaptic Capture

In our earlier study of the VP16-CREB mice, we proposed that the activity of constitutively active CREB led to a cell-wide distribution of CRE-driven gene products in the postsynaptic CA1 neuron that primed the synapses for subsequent synapse-specific capture of L-LTP by a single tetanus, so giving rise to the facilitated L-LTP phenotype. Here, we have shown than *BDNF* is one of these CRE-driven gene products and can, by itself, be responsible for an important component of the facilitated L-LTP. Because facilitated L-LTP in VP16-CREB mice can be equivalent in molecular terms to synaptic capture mediated L-LTP in wild-type animals (Barco et al., 2002; Frey and Morris, 1997), BDNF may also contribute to the processes of synaptic tagging and capture in normal mice. To test this prediction, we carried out two-pathway experiments in slices of *BDNF* heterozygous mice. We stimulated two independent inputs (S1 and S2) to the same CA1 neuronal population and found that synaptic capture was dramatically impaired in *BDNF*$^{+/-}$ mice (Figure 7A, S2, wt: 120–150 min = 147% ± 9%; *BDNF*$^{+/-}$: 114% ± 7%, $p = 0.01$), while 4 × 100 Hz L-LTP was normal (Figure 7A, S1, wt: 120–150 min = 147% ± 12%; *BDNF*$^{+/-}$: 145% ± 18%, $p = 0.88$).

To further explore the role of BDNF in synaptic capture, we used mice in which the genetic deletion was restricted either to the entire forebrain, including both the CA3 and CA1 pyramidal neurons of the hippocampus, or only to the postsynaptic CA1 neurons. Thus, we could assess the individual contributions of pre- and postsynaptic sources of BDNF. We found that both types of *BDNF* mutants had normal 4 × 100 Hz-induced L-LTP in S1 but exhibited a defect in synaptic capture in S2 (Figures 7B and 7C). This defect was more pronounced in the case of the forebrain *BDNF*$^{-/-}$*(CA3-CA1)* mutants, suggesting that BDNF may play a dual role in synaptic capture. First, the decay of the late phase observed in the more restricted *BDNF*$^{-/-}$*(CA1)* mutants suggests a late, postsynaptic role in the maintenance of captured L-LTP (Figure 7C, S2 3 hr after stimulation: 150% ± 7% for wild-type mice and 130% ± 9% for *BDNF*$^{-/-}$*(CA1)* mice, $p = 0.044$), a view consistent with our results in VP16-CREB and *BDNF*$^{+/-}$ mice, with the facilitation of the late phase of LTP by exogenous BDNF (Kovalchuk et al., 2002) and with the late enhancement of BDNF expression observed in postsynaptic CA1 neurons after L-LTP induction (Patterson

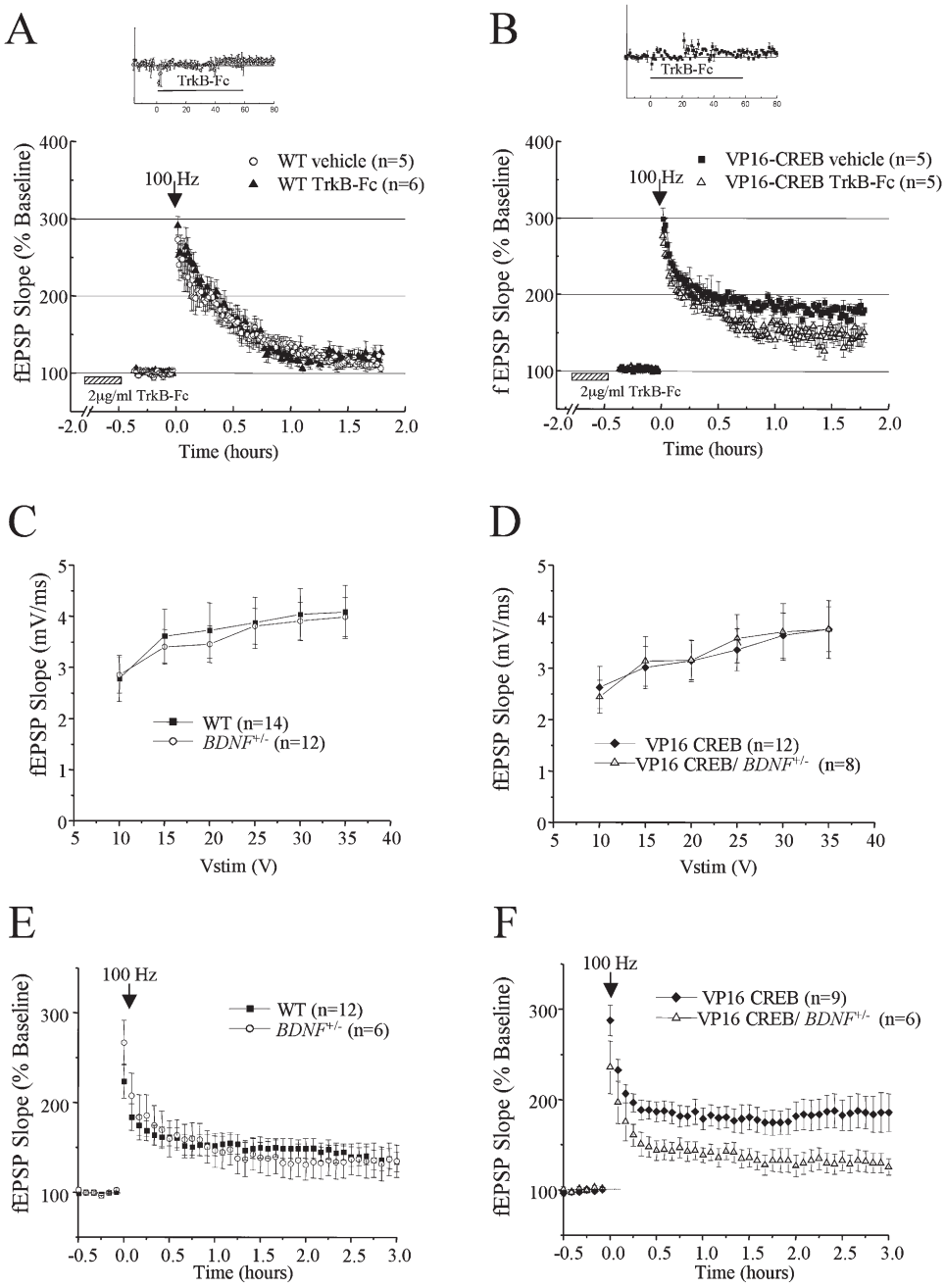

Figure 6. Pharmacological or Genetic Suppression of BDNF Reverses the Facilitated L-LTP Phenotype of VP16-CREB Mice

(A) Exogenous addition of TrkB-Fc had no effect on either test fEPSPs generated at CA3-CA1 synapses (inset) or E-LTP induced by a single tetanus of 100 Hz stimulation in wild-type mice. (B) Exogenous addition of TrkB-Fc had not effect on test fEPSPs generated at CA3-CA1 synapses (inset) but reduced the amplitude of facilitated L-LTP induced by a single tetanus of 100 Hz stimulation in VP16-CREB mice. (C and D) Input-output curves of fEPSP slope (mV/ms) versus stimulus (V) at the Schaffer collateral pathway of hippocampal slices from *BDNF*$^{+/-}$ and control mice or VP16-CREB/*BDNF*$^{+/-}$ double mutant and VP16-CREB mice. (E) Normal E-LTP induced by a single 100 Hz train in *BDNF*$^{+/-}$ and control mice. (F) Facilitated L-LTP evoked by a single 100 Hz train is reduced in VP16-CREB/*BDNF*$^{+/-}$ double mutants. In all panels, results are presented as means ± SEM.

et al., 1992). Second, the rapid decay of captured LTP in slices lacking presynaptic BDNF (Figure 7B, S2 3 hr after stimulation: 161% ± 21% for wild-type mice and 113% ± 8% for *BDNF*$^{-/-}$*(CA3-CA1)* mice, p = 0.019) suggests that the presynaptic release of BDNF into the synaptic cleft after tetanic stimulation may participate in the postsynaptic tagging of the synapse.

Although the role of BDNF in hippocampal LTP has been extensively studied, some aspects of its function are just beginning to be understood. For example, BDNF seems to participate only in some forms of LTP (Korte et al., 1995; Korte et al., 1998; Patterson et al., 1996, 2001; Zakharenko et al., 2003). Also, the presynaptic or postsynaptic source of BDNF and its cellular

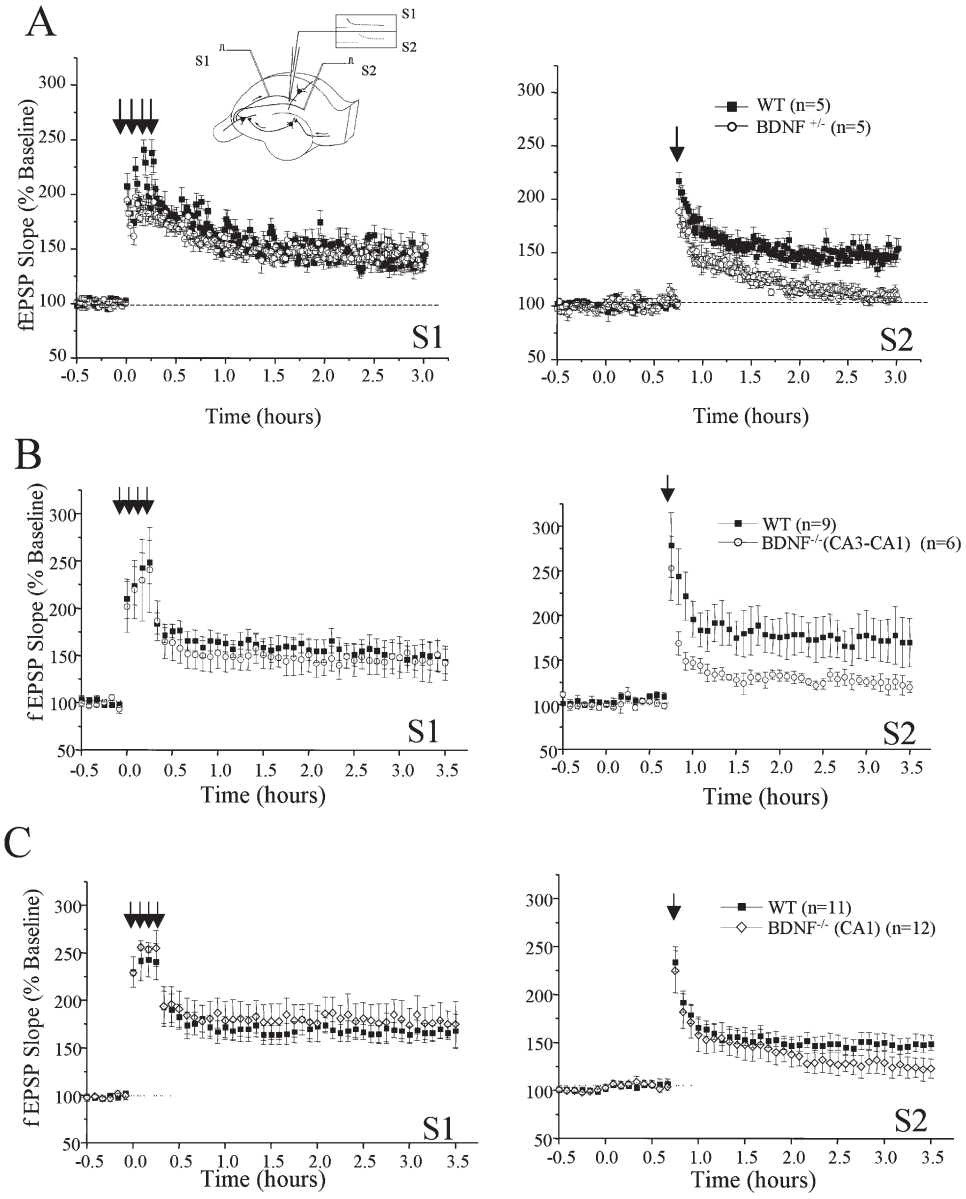

Figure 7. Synaptic Capture in BDNF-Deficient Mice

(Inset) Drawing of a hippocampal slice showing the positioning of the electrodes. Recordings in S1 are represented in the left panels, and recording in S2 are represented in the rigth panels. (A) In wild-type mice, the formation of L-LTP in S1 enables the induction of L-LTP in S2 by 100 Hz stimulation. *BDNF*$^{+/-}$ mice showed a deficit in both the initial amplitude and the duration of synaptic capture-mediated LTP in S2. (B) Genetic disruption of *BDNF* in the CA3 and CA1 regions of the hippocampus significantly reduces the amplitude and duration of synaptic capture-mediated LTP in S2 but does not affect noticeably the expression of L-LTP in S1. (C) Genetic disruption of *BDNF* only in CA1 postsynaptic neurons does not affect the initial amplitude of synaptic capture-mediated LTP in S2 but reduces its late phase. In all panels, results are presented as means ± SEM.

targets in different forms of LTP are only now being delineated (Manabe, 2002; Zakharenko et al., 2003). Our study further clarifies these issues in two ways (Figure 8). First, similarly to experiments using exogenously applied BDNF (Kovalchuk et al., 2002), the experiments in VP16-CREB mice suggest that, regardless of the site of BDNF release, increased levels of BDNF in the synaptic cleft lead to a facilitation of LTP in CA3-CA1 synapses, probably by acting on both pre- and postsynaptic targets. An enhanced release of BDNF accumulated in postsynaptic spines of CA1 neurons of VP16-CREB mice after tetanic stimulation may contribute to sustaining an otherwise transient potentiation by stimulating local protein synthesis (Aakalu et al., 2001; Kang and Schuman, 1996) or enhancing the neurotransmitter release from presynaptic CA3 neurons (Tyler et al., 2002; Tyler and Pozzo-Miller, 2001; Zakharenko et al., 2003). Second, our experiments on synaptic capture suggested distinct roles for pre- or postsynaptically released BDNF. Interestingly, a recent study in neuronal primary cultures has demonstrated that BDNF-induced plasticity exhibits a bimodal profile and has an early

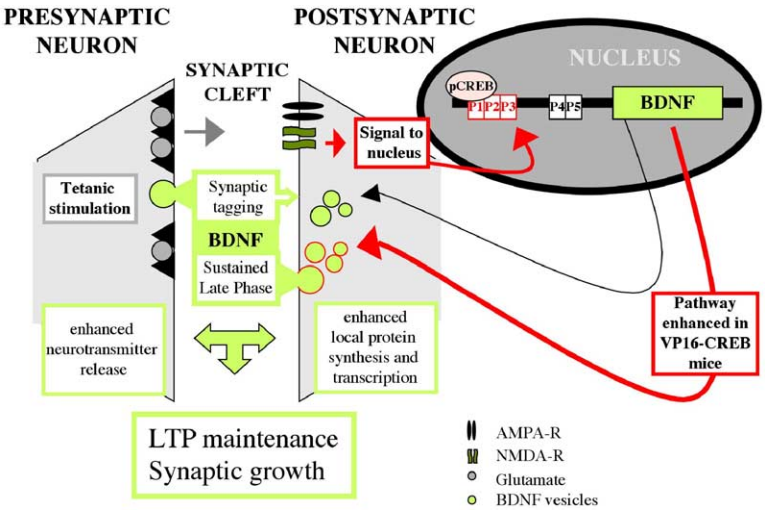

Figure 8. L-LTP Facilitation in VP16-CREB Mice and the Various Roles of BDNF in Synaptic Plasticity

The release of BDNF into the synaptic cleft by the pre- or postsynaptic neuron can stimulate different functions in both the pre- and postsynaptic terminal. Induction of NMDAR-dependent LTP enhances the release of BDNF, which participates in diverse cellular mechanisms related to the maintenance of LTP, such as the stimulation of local protein synthesis in the synapse, the enhancement of neurotransmitter release by the presynaptic neuron, and the activation of transcription in the nucleus of the postsynaptic neuron. These processes contribute to the perpetuation of the, otherwise transient, strengthening of synaptic connections in some forms of LTP. VP16-CREB mice exhibit an enhanced expression of BDNF transcripts bearing exons 1, 2, or 3 in postsynaptic CA1 neurons that enables the rapid establishment of the late phase of LTP observed in these animals. Our results also suggest a role of presynaptically released BDNF in the postsynaptic tagging of the synapse.

presynaptic component and a later postsynaptic component (Alder et al., 2005). Our results indicate that a similar bimodal action can be also observed in hippocampal slices. Thus, presynaptically released BDNF contributes to the formation of those forms of LTP that recruit a presynaptic component (Zakharenko et al., 2003) and might participate in tagging the synapse for subsequent capture of late-phase LTP (this study), while postsynaptically released BDNF might contribute to the maintenance of different forms of L-LTP at late times (Korte et al., 1998; Patterson et al., 2001), including facilitated L-LTP in VP16-CREB mice and synaptically captured L-LTP.

Concluding Remark

LTP is not a unitary phenomenon, but a family of different processes. It is most likely for this reason that hundreds of molecules and more than a dozen molecular pathways have been implicated in the induction, expression, and maintenance of the family of LTP processes. The list of candidate genes revealed by this study suggests the existence of complex interactions between various gene networks. Nevertheless, our analysis provides insights into the molecular mechanism underlying a specific aspect of the phenotype of VP16-CREB mice: their enhanced L-LTP in the Schaffer collateral pathway. We found that the overexpression of BDNF by itself importantly contributes to the L-LTP phenotype of VP16-CREB mice and that reducing BDNF compromises the phenotype. Further physiological studies might reveal the contribution of other candidate genes to other aspects of the complex phenotype of VP16-CREB mice and explain the causes and consequences of their altered expression.

Experimental Procedures

Generation and Maintenance of Transgenic Mice

Generation of *pCaMKII*-tTA, *tetO*-VP16-CREB, *Pdyn*$^{-/-}$, *CD3δ*$^{-/-}$, *BDNF*$^{+/-}$, *BDNF*$^{-/-}$ *(CA3-CA1)*, and *BDNF*$^{-/-}$*(CA1)* mutant mice has been described before (Barco et al., 2002; Ernfors et al., 1994; Love et al., 1993; Mayford et al., 1996; Sharifi et al., 2001; Zakharenko et al., 2003). We designated as VP16-CREB mice those bitransgenic animals that resulted from the crossing of *pCaMKII*-tTA (line B) and *tetO*-VP16-CREB (line VC27) mice. In experiments using VP16-CREB mice, dox was administrated at 40 mg/Kg of food and was removed at specific times before experimentation. Mice were maintained and bred under standard conditions, consistent with NIH guidelines and approved by the IACUC.

Microarrays

Total RNA was extracted from dissected hippocampi or microdissected CA1 regions using TRIzol (Invitrogen) according to the manufacturer's protocol. PolyA mRNA was then isolated using Messagemaker kit (Pharmacia). cDNA synthesis and cRNA production and fragmentation were carried out as described in the Expression Analysis Technical Manual (Affymetrix). U74Av2 gene chips were hybridized, stained, washed, and screened for quality according to the manufacturer's protocol. The Affymetrix gene chip data were processed, normalized, and statistically analyzed using GCOS 1.2 software. The TGT value chosen for the normalization was 500, and each array was normalized according to its baseline (mRNA from the hippocampus or microdissected CA1 regions of wild-type littermates). The scaling factor after normalization was comparable in all arrays. I, D, MI, MD, and NC calls where obtained according to the change threshold defined by the software. We filtered and sorted the list of genes using the *change p value, change call*, and *log ratio signal* as described in the text and figure legends. Subsequent agglomerative hierarchical clustering analysis was performed using the Spotfire DecisionSite for Functional Genomics software (Somerville, MA). We used the UPGMA (unweighted average) clustering method and based the measure of similarity on euclidean distances. Function annotations in Table 1 were generated using the gene ontology browser tool included in the SpotFire software and the ontology information available in NetAffx analysis center.

In Situ Hybridization and Quantitative RT-PCR

Radioactive in situ hybridization was performed as described in Wisden and Morris (1994) with [^{33}P]ATP-labeled oligonucleotides. MHC I transcripts were also detected using DIG-labeled RNA probes and a Tyramide signal amplification kit (Molecular Probes, Eugene, OR). qPCR was carried out in an Applied Biosystems 7300 real-time PCR unit using the *SYBR Premix ex Taq* mix (Takara) and primers specific for the different BDNF exons (Table S2). Each independent sample was assayed in triplicate and *BDNF* levels were normalized using GAPDH.

Electrophysiology

Hippocampi were collected following cervical dislocation of 3- to 4-month-old mice of either sex. Transverse hippocampal slices (400 μm) were incubated in an interface chamber at 27°C–28°C, subfused with oxygenated artificial cerebrospinal fluid (ACSF, containing 119 mM NaCl, 4.0 mM KCl, 1.5 mM $MgSO_4$, 2.5 mM $CaCl_2$, 26.2 mM $NaHCO_3$, 1 mM NaH_2PO_4, and 11 mM mM glucose), and allowed to equilibrate for at least 2 hr. Field excitatory postsynaptic potentials (fEPSP) from the CA1 area were recorded from apical dendrites by placing both stimulating and recording electrodes in the stratum radiatum. Two-pathway experiments were performed by placing two stimulating electrodes and one recording electrode within the stratum radiatum of the CA1 area (see scheme in Figure 7A). The recording electrode could separately detect fEPSPs generated by the activation of the independent pathways activated by each stimulating electrode. We confirmed pathway independence by testing paired-pulse facilitation between each set of afferents (data not shown). Before each experiment, synaptic input/output curves were generated, and the stimulation intensity was adjusted to give fEPSP slopes of approximately 30%–40% of maximum. Baselines were sampled once per minute at this intensity (test pulse, 0.05 ms duration). E-LTP and L-LTP induction protocols consisted, respectively, of one or four (with 5 min intertrain intervals) 1 s train at 100 Hz. the LTD induction protocol consisted of one train of 900 pulses at 1 Hz. When indicated, ACSF was supplemented with dynorphin 1-13 (Sigma) or TrkB-Fc (generous gift of Regeneron). All the electrophysiology experiments, except the time course in Figure 1A, were carried out 2 weeks after dox removal. At this time postinduction, two-photon microscopy confirmed that spine morphology in CA1 neurons was normal in VP16-CREB mice (C. Lang et al., personal communication). Two-way ANOVA and Student's t test were used for data analysis. In the text, the electrophysiological data are presented as mean ± SD, whereas in the figures the values are presented as mean ± SEM and the number of tested slices is indicated in brackets. Experimenters were blind to mice genotype.

Supplemental Data

The Supplemental Data for this article can be found online at http://www.neuron.org/cgi/content/full/48/1/123/DC1/.

Acknowledgments

We thank Ute Hochgeschwender (Oklahoma Medical Research Foundation) for providing *Pdyn*$^{-/-}$ mice. We also thank Bing Liu, DeQi Yin, and Román Olivares for excellent technical assistance with genetically modified mice; and Stas Zakharenko and Mikel Lopez de Armentia for critical reading of the manuscript. A.B. was supported by a grant from the Hereditary Disease Foundation and is now supported, together with P.G., by the Marie Curie Excellence grant MEXT-CT-2003-509550. E.R.K is supported by Howard Hughes Medical Institute and by the G. Harold and Leila Y. Mathers Foundation. The authors have declared a conflict of interest. For details, see the Supplemental Data.

Received: January 10, 2005
Revised: July 21, 2005
Accepted: September 1, 2005
Published: October 5, 2005

References

Aakalu, G., Smith, W.B., Nguyen, N., Jiang, C., and Schuman, E.M. (2001). Dynamic visualization of local protein synthesis in hippocampal neurons. Neuron *30*, 489–502.

Alder, J., Thakker-Varia, S., Crozier, R.A., Shaheen, A., Plummer, M.R., and Black, I.B. (2005). Early presynaptic and late postsynaptic components contribute independently to brain-derived neurotrophic factor-induced synaptic plasticity. J. Neurosci. *25*, 3080–3085.

Barco, A., Alarcon, J.M., and Kandel, E.R. (2002). Expression of constitutively active CREB protein facilitates the late phase of long-term potentiation by enhancing synaptic capture. Cell *108*, 689–703.

Barco, A., Pittenger, C., and Kandel, E.R. (2003). CREB, memory enhancement and the treatment of memory disorders: promises, pitfalls and prospects. Expert Opin. Ther. Targets *7*, 101–114.

Bito, H., Deisseroth, K., and Tsien, R.W. (1996). CREB phosphorylation and dephosphorylation: a Ca(2+)- and stimulus duration-dependent switch for hippocampal gene expression. Cell *87*, 1203–1214.

Boulanger, L.M., and Shatz, C.J. (2004). Immune signalling in neural development, synaptic plasticity and disease. Nat. Rev. Neurosci. *5*, 521–531.

Boulanger, L.M., Huh, G.S., and Shatz, C.J. (2001). Neuronal plasticity and cellular immunity: shared molecular mechanisms. Curr. Opin. Neurobiol. *11*, 568–578.

Carlezon, W.A., Jr., Thome, J., Olson, V.G., Lane-Ladd, S.B., Brodkin, E.S., Hiroi, N., Duman, R.S., Neve, R.L., and Nestler, E.J. (1998). Regulation of cocaine reward by CREB. Science *282*, 2272–2275.

Caudle, R.M., Chavkin, C., and Dubner, R. (1994). Kappa 2 opioid receptors inhibit NMDA receptor-mediated synaptic currents in guinea pig CA3 pyramidal cells. J. Neurosci. *14*, 5580–5589.

Cole, R.L., Konradi, C., Douglass, J., and Hyman, S.E. (1995). Neuronal adaptation to amphetamine and dopamine: molecular mechanisms of prodynorphin gene regulation in rat striatum. Neuron *14*, 813–823.

Collins-Hicok, J., Lin, L., Spiro, C., Laybourn, P.J., Tschumper, R., Rapacz, B., and McMurray, C.T. (1994). Induction of the rat prodynorphin gene through Gs-coupled receptors may involve phosphorylation-dependent derepression and activation. Mol. Cell. Biol. *14*, 2837–2848.

Corriveau, R.A., Huh, G.S., and Shatz, C.J. (1998). Regulation of class I MHC gene expression in the developing and mature CNS by neural activity. Neuron *21*, 505–520.

Ernfors, P., Lee, K.F., and Jaenisch, R. (1994). Mice lacking brain-derived neurotrophic factor develop with sensory deficits. Nature *368*, 147–150.

Frey, U., and Morris, R.G. (1997). Synaptic tagging and long-term potentiation. Nature *385*, 533–536.

Hayes, V.Y., Towner, M.D., and Isackson, P.J. (1997). Organization, sequence and functional analysis of a mouse BDNF promoter. Brain Res. Mol. Brain Res. *45*, 189–198.

Huh, G.S., Boulanger, L.M., Du, H., Riquelme, P.A., Brotz, T.M., and Shatz, C.J. (2000). Functional requirement for class I MHC in CNS development and plasticity. Science *290*, 2155–2159.

Impey, S., Mark, M., Villacres, E.C., Poser, S., Chavkin, C., and Storm, D.R. (1996). Induction of CRE-mediated gene expression by stimuli that generate long-lasting LTP in area CA1 of the hippocampus. Neuron *16*, 973–982.

Impey, S., Smith, D.M., Obrietan, K., Donahue, R., Wade, C., and Storm, D.R. (1998). Stimulation of cAMP response element (CRE)-mediated transcription during contextual learning. Nat. Neurosci. *1*, 595–601.

Ishiguro, N., Brown, G.D., Ishizu, A., and Meruelo, D. (1998). The regulation of murine H-2Dd expression by activation transcription factor 1 and cAMP response element binding protein. J. Immunol. *160*, 5907–5914.

Kang, H., and Schuman, E.M. (1996). A requirement for local protein synthesis in neurotrophin-induced hippocampal synaptic plasticity. Science *273*, 1402–1406.

Korte, M., Carroll, P., Wolf, E., Brem, G., Thoenen, H., and Bonhoeffer, T. (1995). Hippocampal long-term potentiation is impaired in mice lacking brain-derived neurotrophic factor. Proc. Natl. Acad. Sci. USA *92*, 8856–8860.

Korte, M., Kang, H., Bonhoeffer, T., and Schuman, E. (1998). A role for BDNF in the late-phase of hippocampal long-term potentiation. Neuropharmacology *37*, 553–559.

Kovalchuk, Y., Hanse, E., Kafitz, K.W., and Konnerth, A. (2002).

Postsynaptic induction of BDNF-mediated long-term potentiation. Science *295*, 1729–1734.

Lonze, B.E., and Ginty, D.D. (2002). Function and regulation of CREB family transcription factors in the nervous system. Neuron *35*, 605–623.

Love, P.E., Shores, E.W., Johnson, M.D., Tremblay, M.L., Lee, E.J., Grinberg, A., Huang, S.P., Singer, A., and Westphal, H. (1993). T cell development in mice that lack the zeta chain of the T cell antigen receptor complex. Science *261*, 918–921.

Lu, B. (2003). BDNF and activity-dependent synaptic modulation. Learn. Mem. *10*, 86–98.

Manabe, T. (2002). Does BDNF have pre- or postsynaptic targets? Science *295*, 1651–1653.

Martinowich, K., Hattori, D., Wu, H., Fouse, S., He, F., Hu, Y., Fan, G., and Sun, Y.E. (2003). DNA methylation-related chromatin remodeling in activity-dependent BDNF gene regulation. Science *302*, 890–893.

Mayford, M., Bach, M.E., Huang, Y.Y., Wang, L., Hawkins, R.D., and Kandel, E.R. (1996). Control of memory formation through regulated expression of a CaMKII transgene. Science *274*, 1678–1683.

Patterson, S.L., Grover, L.M., Schwartzkroin, P.A., and Bothwell, M. (1992). Neurotrophin expression in rat hippocampal slices: a stimulus paradigm inducing LTP in CA1 evokes increases in BDNF and NT-3 mRNAs. Neuron *9*, 1081–1088.

Patterson, S.L., Abel, T., Deuel, T.A., Martin, K.C., Rose, J.C., and Kandel, E.R. (1996). Recombinant BDNF rescues deficits in basal synaptic transmission and hippocampal LTP in BDNF knockout mice. Neuron *16*, 1137–1145.

Patterson, S.L., Pittenger, C., Morozov, A., Martin, K.C., Scanlin, H., Drake, C., and Kandel, E.R. (2001). Some forms of cAMP-mediated long-lasting potentiation are associated with release of BDNF and nuclear translocation of Phospho-MAP kinase. Neuron *32*, 123–140.

Sharifi, N., Diehl, N., Yaswen, L., Brennan, M.B., and Hochgeschwender, U. (2001). Generation of dynorphin knockout mice. Brain Res. Mol. Brain Res. *86*, 70–75.

Shieh, P.B., and Ghosh, A. (1999). Molecular mechanisms underlying activity-dependent regulation of BDNF expression. J. Neurobiol. *41*, 127–134.

Shukla, V.K., and Lemaire, S. (1994). Non-opioid effects of dynorphins: possible role of the NMDA receptor. Trends Pharmacol. Sci. *15*, 420–424.

Tabuchi, A., Nakaoka, R., Amano, K., Yukimine, M., Andoh, T., Kuraishi, Y., and Tsuda, M. (2000). Differential activation of brain-derived neurotrophic factor gene promoters I and III by Ca2+ signals evoked via L-type voltage-dependent and N-methyl-D-aspartate receptor Ca2+ channels. J. Biol. Chem. *275*, 17269–17275.

Tabuchi, A., Sakaya, H., Kisukeda, T., Fushiki, H., and Tsuda, M. (2002). Involvement of an upstream stimulatory factor as well as cAMP-responsive element-binding protein in the activation of brain-derived neurotrophic factor gene promoter I. J. Biol. Chem. *277*, 35920–35931.

Tao, X., Finkbeiner, S., Arnold, D.B., Shaywitz, A.J., and Greenberg, M.E. (1998). Ca2+ influx regulates BDNF transcription by a CREB family transcription factor-dependent mechanism. Neuron *20*, 709–726.

Tao, X., West, A.E., Chen, W.G., Corfas, G., and Greenberg, M.E. (2002). A calcium-responsive transcription factor, CaRF, that regulates neuronal activity-dependent expression of BDNF. Neuron *33*, 383–395.

Taubenfeld, S.M., Wiig, K.A., Bear, M.F., and Alberini, C.M. (1999). A molecular correlate of memory and amnesia in the hippocampus. Nat. Neurosci. *2*, 309–310.

Terman, G.W., Wagner, J.J., and Chavkin, C. (1994). Kappa opioids inhibit induction of long-term potentiation in the dentate gyrus of the guinea pig hippocampus. J. Neurosci. *14*, 4740–4747.

Timmusk, T., Palm, K., Lendahl, U., and Metsis, M. (1999). Brain-derived neurotrophic factor expression in vivo is under the control of neuron-restrictive silencer element. J. Biol. Chem. *274*, 1078–1084.

Timmusk, T., Palm, K., Metsis, M., Reintam, T., Paalme, V., Saarma, M., and Persson, H. (1993). Multiple promoters direct tissue-specific expression of the rat BDNF gene. Neuron *10*, 475–489.

Tyler, W.J., and Pozzo-Miller, L.D. (2001). BDNF enhances quantal neurotransmitter release and increases the number of docked vesicles at the active zones of hippocampal excitatory synapses. J. Neurosci. *21*, 4249–4258.

Tyler, W.J., Perrett, S.P., and Pozzo-Miller, L.D. (2002). The role of neurotrophins in neurotransmitter release. Neuroscientist *8*, 524–531.

Wagner, J.J., Terman, G.W., and Chavkin, C. (1993). Endogenous dynorphins inhibit excitatory neurotransmission and block LTP induction in the hippocampus. Nature *363*, 451–454.

Wisden, W., and Morris, B.J. (1994). In situ hybridization with synthetic oligonucleotide probes. In In Situ Hybridization Protocols for the Brain, W. Wisden and B.J. Morris, eds. (London: Elsevier Science), pp. 4–56.

Zakharenko, S.S., Patterson, S.L., Dragatsis, I., Zeitlin, S.O., Siegelbaum, S.A., Kandel, E.R., and Morozov, A. (2003). Presynaptic BDNF required for a presynaptic but not postsynaptic component of LTP at hippocampal CA1–CA3 synapses. Neuron *39*, 975–990.